Acta Scientiarum. Technology
ISSN: 1806-2563
ISSN: 1807-8664
actatech@uem.br
Universidade Estadual de Maringá
Brasil

Optimizing production in machining of hardened steels using response surface methodology

Campos, Paulo Henrique da Silva; Paes, Vinicius de Carvalho; Gonçalves, Ernany Daniel de Carvalho; Ferreira, João Roberto; Balestrassi, Pedro Paulo; Davim, João Paulo
Optimizing production in machining of hardened steels using response surface methodology
Acta Scientiarum. Technology, vol. 41, 2019
Universidade Estadual de Maringá, Brasil
Available in: https://www.redalyc.org/articulo.oa?id=303260200041
DOI: https://doi.org/10.4025/actascitechnol.v41i1.38091

Estatística

Optimizing production in machining of hardened steels using response surface methodology

Paulo Henrique da Silva Campos
Universidade Federal de Itajubá, Brasil

Vinicius de Carvalho Paes
Universidade Federal de Itajubá, Brasil
viniciuspaes@gmail.com

Ernany Daniel de Carvalho Gonçalves
Universidade Federal de Itajubá, Brasil

João Roberto Ferreira
Universidade Federal de Itajubá, Brasil

Pedro Paulo Balestrassi
Universidade Federal de Itajubá, Brasil

João Paulo Davim
Universidade de Aveiro, Brasil

DOI: https://doi.org/10.4025/actascitechnol.v41i1.38091
Redalyc: https://www.redalyc.org/articulo.oa?id=303260200041

Received: 10 July 2017
Accepted: 08 February 2018

Abstract:

This paper presents the modeling of tool life and surface roughness for machining AISI 52100 steel with a hardness of 50 HRC through Design of Experiments and Response Surface Methodology (RSM) with a view to enhance the quality and productivity. Knowing that the tool life and surface roughness are factors that influence the quality of the product, this study used the statistical tool of RSM in the search of factors that better determine optimal models. The models obtained prioritize the product quality and the cutting productivity. Results from Analysis of Variance demonstrated that the mathematical models elaborated allowed the prediction of surface roughness parameters' values and tool life (T) with a precision of 95% confidence interval and a coefficient of determination above 94%. The wiper geometry of the tool led to the achievement of low average surface roughness (Ra) ranging from 0.2 to 0.4 μm with relatively high advances (0.2-0.4 mm rev^{-1}) and maximum height of the profile surface roughness (Rt) in the range of 1.4 to 2.8 μm, without making use of the cutting fluid.

Keywords: design of experiments, response surface methodology, production optimization.

Introduction

Turning and hard turning technology has become an important manufacturing process and is used in a great variety of industrial applications like shafts, cams, bearings, forged parts, molds and dies (Davim, 2011). In the machining process, in order to make the parts that will provide the correct functioning, it is necessary to reach the desired surface quality. According to Shihab, Khan, Mohammad, and Siddiqueed (2014a), the hard machining presents challenges to attain high-precision machining and improved tool life in terms of

Author notes

viniciuspaes@gmail.com

selection of tool insert. The process in hard turning differs from conventional turning basically because of the characteristics: cutting tool, mechanisms involved during chip formation, and workpiece hardness. Grzesik and Zak (2012) and Grzesik and Wanat (2006) also points some advantages of hard turning: the cutting of production costs, reduction of each operation's processing time, and elimination of the need for cutting fluid.

Production cost and the performance of the overall mechanical system is greatly influenced by the surface roughness, so this characteristic is very significant as a quality measure. Ferreira, Řehoř, Lauro, Carou, and Davim (2016) analyzed the flank wear and its influence on the resulting surface roughness in hard turning processes of AISI H13 machined parts with ceramic tools and found that cutting speed exerted a significant influence on the flank wear, but there were no clear trends of surface roughness with tool wear, either with or without wiper tools.

According to Zhang, Liu, and Yao (2007), improved surface roughness can be achieved with wiper inserts or increased feed rates; so, it is possible to achieve better surface finish or increase the productivity with hard part machining. In Suleyman, Yaldiz, and Turkes (2011), the influence of tool geometry on the surface finish in hard turning was researched; the Response Surface Methodology (RSM) was applied and a prediction model was developed related to the Ra. The results indicated that the significant factor to determine Ra and Rt was the tool nose radius.

There is also an alternative hybrid approach, combining Response Surface Methodology (RSM) and Principal Component Analysis to optimize multiple correlated responses during a turning process (Paiva, Ferreira, & Balestrassi, 2007). Scandiffio, Diniz, and Souza (2016) investigated the free-form milling of hard materials employing a ball-end cemented carbide cutting tool and concluded that tool life shortens as the tool vibration levels grow, hard materials cutting stability is improved when the tool tip's center is engaged, thus leading to better quality surface finishing and longer tool life. In addition, Chinchanikar and Choudhury (2015) present a systematic literature review on hard steels machining using coated tools, hard turning, cooling methods and modeling of machining processes.

In this study, RSM was used to find the optimum values of the cutting parameters on the turning of AISI 52100 steel with Al2O3/TiC tool with wiper geometry through the development of a mathematical model of T, Ra and Rt parameters.

Material and methods

The development of Design of Experiments (DOE) was done in the 1920's and later has been enhanced and applied by leading researchers all around the world (Taguchi, 1987).

According to Montgomery (2008), DOE is a methodology used to assess the magnitude and direction of many sources of factors that influence a process, be it a manufacturing one, the design of a new product and/or of a new service. The practitioner should start with the identification of factors and their combinations that may contribute to changes in the model that attempts to describe the behavior of the dependent variables or outcomes. Once the experiments are performed, the analysis proceeds to estimate the main effects of each factor as well as the two-factor (or more) interactions' ones using appropriate statistical methods, which ultimately leads to the screening of factors.

During the conduction of experiments, all the factors are, in general, changed simultaneously and the several ways to combine them are called arrangements or designs. The most general case is the complete or full factorial arrangement; the total number of experiments N is related to the number of factors k by the relation N = 2k. According to Montgomery (2008), all possible combinations of levels of the experimental factors are used in a full factorial DOE technique, thus covering the entire experimental space. The RSM is a specific type of DOE that incorporate optimization techniques. Myers (1999) presented a thorough discussion of the RSM and a historical review of the state-of-the-art of RSM, as well as some suggestions for future research.

Pontes et al. (2010), in their concern with surface roughness in hard turning, proved that DOE is an efficient predictive statistical tool when designing Artificial Neural Networks of Radial Basis Function architectures. Santhanakumar, Adalarasan, Siddharth, and Velayudham (2016) employed a grey-based RSM and Taguchi's L27 orthogonal design on the study of the influence of cutting speed (Vc), feed rate (f) and depth of cut (ap) on tool's flank wear and on roughness in rough machining of high-strength materials; at the same time they reduced their multi-response optimization case to a single-response one, they found that, even though the surface finish's quality was improved by the increase of the cutting speed, as feed rate and depth of cut increase to elevated values the roughness also increased.

According to Bouacha, Yallese, Khamel, and Belhadi (2014), the AISI 52100 hardened steel (the same material used for the experiments in this paper) is highly recommended for the manufacture of various profiling rollers, balls, dies and bearing cages. It is also recommended in cold working, for profiling cylinders, forming matrices and for wear coating purposes.

The dimensions of the steel rod used in this research were: diameter = 49 and length = 50 mm. The chemical composition of the AISI 52100 steel (in wt. %) is described in Table 1.

A CNC machine was used in the turning process, with maximum power of 7.5 HP axis; maximum speed of 4,000 rpm; maximum torque of 200 kgf m^{-1} and a turret with eight positions.

The inserts are of mixed ceramic (Al2O3 + TiC) coated with titanium nitride (TiN), GC 6050 class with wiper geometry ISO CNGA S01525WH 120408. The tool holder is ISO DCLNL Model 1616H12; position angle of 95°, rake angle of -6° and clearance angle of 7°.

TABLE 1.
AISI 52100 steel chemical composition.

Iron (Fe)	Carbon (C)	Silicon (Si)
96.83%	1.03%	0.23%
Manganese (Mn)	Chromium (Cr)	Molybdenum (Mo)
0.35%	1.40%	0.04%
Nitrate (Ni)	Sulfur (S)	Phosphorous (P)
0.11%	0.00%	0.01%

The tool wear was monitored using an optical microscope with a digital camera at 40x magnification. The permissible flank wear was established at VBB = 0.3 mm. Measuring Ra and Rt a tool tip was used. Roughness measurements were made using a portable stylus-type profilometer, Surtronic 3+ stylus-type instrument manufactured by Taylor Hobson. The roughness measurements were taken at three different points of the piece and four values per point were measured, totaling twelve measures for each run accomplished.

The criterion for tool change, especially roughness values (Ra < 0.5) μm, was flank wear VBB < 0.3 mm. This criterion was adopted according to the risk of breakage of the mixed ceramic insert and each piece machined was removed so the roughness could be measured. Moreover, the insert was removed from toolholder for monitoring the flank wear (VBB). Figure 1a shows the tool wear mixed ceramic and Figure 1b the hard turning process of AISI 52100 steel used in the experimental study.

In the 2k full factorial design, each input factor has two levels; the total of experiments are related to the total possible combinations between factors. After the full factorial analysis, the design was augmented through the addition of axial points, to form a central composite design (CCD) of the RSM. All the analysis was based on Minitab® numerical results.

In running a two-level factorial, the practitioner may start by fitting the first-order model with interactions of Equation 1-2 for exploratory reasons; however, the second-order model of Equation 3 is frequently more adequate. There is the possibility of replicating certain points in a 2k factorial that gives useful information about the curvature in the experimental region. The method consists of adding center points to the 2k design. The important reason for including the center points at the design is that they do not affect the effect estimates in a 2k design (Gheshlaghi, Scharer, Moo-Young, & Douglas, 2008). Based on that, the turning tests were evaluated in a way to provide accuracy when studying the correlation of cutting parameters on machining tool life and workpiece roughness through the application of factorial and response surface designs. Table 2 lists the setup of the experiment.

$$y = \beta_0 + \sum_{i=1}^{k} \beta_i x_i + \varepsilon \quad (1)$$ (1)

$$y = \beta_0 + \sum_{i=1}^{k} \beta_i x_i + \sum_{i<j} \sum^{k} \beta_{ij} x_i x_j + \varepsilon \quad (2)$$ (2)

$$y = \beta_0 + \sum_{i=1}^{k} \beta_i x_i + \sum_{i=1}^{k} \beta_{ii} x_i^2 + \sum_{i<j} \sum^{k} \beta_{ij} x_i x_j + \varepsilon \quad (3)$$ (3)

The guidelines, hardness of the workpiece material and the chemical composition provided by the cutting tool manufacturer inspired the selection of these levels.

The most used response surface experimental approach is the CCD. As stated, it consists of a factorial design with center points, allowing an efficient estimation of first and second-order terms augmented with a group of axial points (Montgomery, 2008). Table 3 presents the experimental matrix using the levels defined in Table 2 and the measured responses.

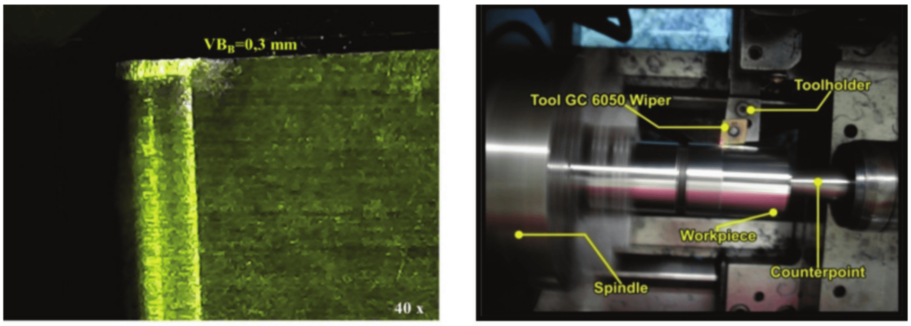

(a) (b)

FIGURE 1.
Process of hard turning with mixed carbide ceramics.

It is of crucial importance to confirm the adequacy of each fitted model; the criteria to select the most adequate model are based on the lack-of-fit test and the adjusted coefficient of determination, R^2adj, which is a modified R^2 that is adjusted for the number of terms in the model (Ohale, Uzoh, & Onukwuli, 2017). Four types of models have been employed in this study using Equation 1-3: (a) linear, (b) linear + interactions, (c) linear + squares and (d) full quadratic models were specified.

When unnecessary terms are included, R^2 can be artificially high. Unlike R^2, R^2adj may get smaller when unnecessary terms are added to the model. Table 4 shows the results for the four models that were fitted to T, Ra and Rt; see also Figure 2, which illustrates the average response surface for Ra using Equation 1-7; the analysis of the response surface for the average roughness as a function of Vc, f and ap presents evidences that the factor that most influences the Ra of the machined surface is f. In this way, it is also possible to verify visually by analyzing the surfaces that the increase of f impacts on the increase of Ra; the increase of Vc impact to increase Ra.

Residual analysis aims to assess the quality of results, in other words, show whether the results are real or whether they are coincidental. In addition, it serves to identify discrepancies or errors, such as inversion of values, misspellings, inadequacy of the experiment result, and so on. According to Montgomery (2008), when a model is properly formulated, the residual should not be correlated (independent) and should be normally distributed.

TABLE 2.
Cutting Parameters and their levels.

Symbol	Unit	Factor levels				
		-1.68	-1	0	+1	1.68
Vc	m min.$^{-1}$	186	200	220	240	254
f	mm rev^{-1}	0.13	0.20	0.30	0.40	0.46
ap	mm	0.09	0.15	0.22	0.30	0.35

TABLE 3.
Central composite design.

Vc m min.$^{-1}$	f mm rev^{-1}	ap mm	A	B	C	T min.	Ra µm	Rt µm
200	0.20	0.15	-1	-1	-1	17.21	0.255	1.416
240	0.20	0.15	1	-1	-1	11.37	0.276	1.456
200	0.40	0.15	-1	1	-1	5.96	0.317	2.121
240	0.40	0.15	1	1	-1	4.48	0.307	2.159
200	0.20	0.30	-1	-1	1	9.42	0.255	1.456
240	0.20	0.30	1	-1	1	7.37	0.255	1.580
200	0.40	0.30	-1	1	1	4.03	0.351	2.019
240	0.40	0.30	1	1	1	6.10	0.289	1.990
220	0.30	0.22	0	0	0	4.89	0.269	1.818
220	0.30	0.22	0	0	0	5.0	0.259	1.718
220	0.30	0.22	0	0	0	4.77	0.260	1.718
220	0.30	0.22	0	0	0	5.01	0.260	1.722
220	0.30	0.22	0	0	0	5.12	0.260	1.718
186	0.30	0.22	-1.68	0	0	9.51	0.290	1.694
254	0.30	0.22	1.68	0	0	6.86	0.260	1.818
220	0.13	0.22	0	-1.68	0	14.18	0.217	1.549
220	0.46	0.225	0	1.68	0	4.12	0.317	2.549
220	0.30	0.100	0	0	-1.68	9.42	0.317	1.946
220	0.30	0.350	0	0	1.68	4.92	0.317	1.746

TABLE 4.
Selection of the best model in Response Surface Design.

Model	T		Ra		Rt	
	R^2_{adj}	lack-of-fit test	R^2_{adj}	lack-of-fit test	R^2_{adj}	lack-of-fit test
Linear	62,51%	0.000	53.66%	0.001	83.18%	0.024
Linear + Interactions	73.15%	0.000	57.18%	0.001	81.78%	0.018
Linear + Squares	79.79%	0.000	83.17%	0.009	90.65%	0.063
Full Quadratic	99.74%	0.172	97.69%	0.286	91.26%	0.059

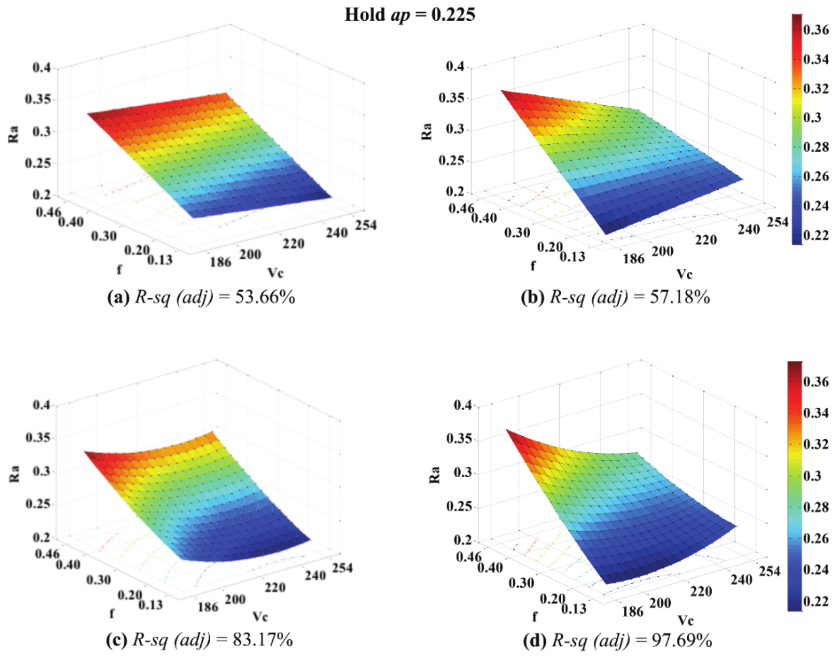

FIGURE 2.
Response surfaces for Ra using models (a) linear; (b) linear + interactions; (c) linear + squares and; (d) full quadratic.

$$Ra_{linear} = 0.280568 - 0.007383 * Vc + 0.028595 * f - 0.000300 * ap \quad (4)$$ (4)

$$Ra_{linear+interactions} = 0.280568 - 0.007383Vc + 0.028595 * f - 0.0003000 * ap - 0.011720 * Vc * f - 0.009314 * Vc * ap + 0.004484 * f * ap \quad (5)$$ (5)

$$Ra_{linear+squares} = 0.261628 - 0.007383 * Vc + 0.028595 * f - 0.0003000 * ap + 0.004750 * Vc^2 + 0.001991 * f^2 + 0.019608 * ap^2 \quad (6)$$ (6)

Results and discussion

Table 5 lists the measurements considering a full factorial design with eight corners and five center points. Analysis of variance (ANOVA) was applied to investigate the main effects, interactions and curvature effects of T, Ra and Rt (see Table 6, 7 and 8, respectively).

The non-significance of the various terms was assessed on the basis of the resultant P-values: (a) in the case of T, the three-way interaction Vc * f * ap (p = 0.558), (b) in the case of Ra, both the main effect ap (p = 0.710) and (c) the three-way interaction Vc * f * ap (p = 0.057). In the case of Rt, that just the main effect f and two-effect f * ap were significant (p = 0.000 and 0.025, respectively).

Curvature tests indicate that the center points added to the experimental matrix provided statistical evidence of curvature for the response surfaces T and Ra. In addition, Figure 3 shows graphically the main and curvature effects for each response and Figures 4, 5 and 6 shows the effect of interactions of controllable variables on responses.

It is essential to realize that the factor f has the greater main effect in each response, due to the steeper slope than the other factors. In Figure 3a, the difference (ycorner - ycenter) is small, that is the reason why the center points are lying near the plane passing through the factorial points. The almost horizontal behaviors for factors ap in Figure 3b as well as Vc and ap in Figure 3c show that there is no significant impact on the responses when the levels are changed from the low to the high.

According to the results in Table 4, the full quadratic model is the most appropriate approach to fit the response surfaces for T, Ra and Rt: R^2adj = 99.74, 97.69 and 91.26%, respectively. Table 9, 10 and 11 present the ANOVA results for each response. Despite the fact that some terms are not significant, mainly for Rt, if any one of them is removed, either R^2adj or the lack-of-fit test indicates a worsening of the model. As stated, removing these terms of Rt, the new R^2adj = 82.00% and the lack-of-fit = 0.021. The lack-of-fit P-value indicates that there is 17.2% chance that a 'lack of fit F-value' of 2.78 could occur due to noise, as show in Table 9 (Shihab, Khan, Mohammad, & Siddiqueed, 2014b).

Taking into account Table 4 and the abovementioned analysis, response surfaces and contour plots were generated for T, Ra and Rt, using the full quadratic model in Equation 7 - 9 (see Figure 7); only the most significant variables were generated in the graphs.

$$\mathrm{Ra}_{full\ quadratic} = 0.261628 - 0.007383 * \mathrm{Vc} + 0.028595 * \mathrm{f} - 0.0003000 * \mathrm{ap} + 0.004750 * \mathrm{Vc}^2 + 0.001991 * \mathrm{f}^2 + 0.019608 * \mathrm{ap}^2 - 0.011720 * \mathrm{Vc} * \mathrm{f} - 0.009314 * \mathrm{Vc} * \mathrm{ap} + 0.004484 * \mathrm{f} * \mathrm{ap} \quad (7) \tag{7}$$

$$\mathrm{T}_{full\ quadratic} = 4.9627 - 0.8609 * \mathrm{Vc} - 3.0548 * \mathrm{f} - 1.4402 * \mathrm{ap} + 1.1152 * \mathrm{Vc}^2 + 1.4564 * \mathrm{f}^2 + 0.7564 * \mathrm{ap}^2 + 1.0600 * \mathrm{Vc} * \mathrm{f} + 0.9175 * \mathrm{Vc} * \mathrm{ap} + 1.4350 * \mathrm{f} * \mathrm{ap} \quad (8) \tag{8}$$

$$\mathrm{Rt}_{\mathrm{full\ quadratic}} = 1.74353 + 0.02789 * \mathrm{Vc} + 0.29750 * \mathrm{f} - 0.03252 * \mathrm{ap} - 0.01917 * \mathrm{Vc}^2 + 0.08449 * \mathrm{f}^2 + 0.01270 * \mathrm{ap}^2 - 0.01940 * \mathrm{Vc} * \mathrm{f} + 0.00218 * \mathrm{Vc} * \mathrm{ap} - 0.05446 * \mathrm{f} * \mathrm{ap} \quad (9) \tag{9}$$

TABLE 5.
Full factorial design with five center points.

Vc	f	ap	A	B	C	T	Ra	Rt
200	0.20	0.15	-1	-1	-1	17.21	0.255	1.416
240	0.20	0.15	1	-1	-1	11.37	0.276	1.456
200	0.40	0.15	-1	1	-1	5.96	0.317	2.121
240	0.40	0.15	1	1	-1	4.48	0.307	2.159
200	0.20	0.30	-1	-1	1	9.42	0.255	1.456
240	0.20	0.30	1	-1	1	7.37	0.255	1.580
200	0.40	0.30	-1	1	1	4.03	0.351	2.019
240	0.40	0.30	1	1	1	6.10	0.289	1.990
220	0.30	0.22	0	0	0	4.89	0.269	1.818
220	0.30	0.22	0	0	0	5.0	0.259	1.718
220	0.30	0.22	0	0	0	4.77	0.260	1.718
220	0.30	0.22	0	0	0	5.01	0.260	1.722
220	0.30	0.22	0	0	0	5.12	0.260	1.718

TABLE 6.
ANOVA results for T.

Source	DF	Seq SS	Adj SS	Adj MS	F	P
Main Effects	3	101.843	101.842	33.947	1921.19	0.000
Vc	1	6.661	6.661	6.661	376.98	0.000
f	1	76.880	76.880	76.880	4350.88	0.000
ap	1	18.301	18.301	18.301	1035.72	0.000
2-Way Int.	3	32.197	32.197	10.732	607.38	0.000
Vc*f	1	8.989	8.989	8.988	508.70	0.000
Vc*ap	1	6.734	6.734	6.734	381.12	0.000
f*ap	1	16.474	16.474	16.473	932.30	0.000
3-Way Int.	1	0.007	0.007	0.007	0.41	0.558
Vc*f*ap	1	0.007	0.007	0.007	0.41	0.558
Curvature	1	33.194	33.194	33.193	1878.53	0.000
Residual Error	4	0.071	0.071	0.017		
Pure Error	4	0.071	0.071	0.017		
Total	12	167.311				

Table 7

Source	DF	Seq SS	Adj SS	Adj MS	F	P
Main Effects	3	0.006	0.006	0.002	127.77	0.000
Vc	1	0.000	0.000	0.000	18.75	0.012
f	1	0.006	0.006	0.006	364.40	0.000
ap	1	0.000	0.000	0.000	0.16	0.710
2-Way Int.	3	0.001	0.002	0.000	38.41	0.002
Vc*f	1	0.001	0.001	0.001	64.81	0.001
Vc*ap	1	0.001	0.001	0.001	40.93	0.003
f*ap	1	0.000	0.00	0.000	9.49	0.037
3-Way Int.	1	0.000	0.000	0.000	7.01	0.057
Vc*f*ap	1	0.000	0.000	0.000	7.01	0.057
Curvature	1	0.002	0.002	0.002	127.91	0.000
Residual Error	4	0.000	0.000	0.000		
Pure Error	4	0.000	0.000	0.000		
Total	12	0.011				

ANOVA results for Ra.

TABLE 8.
ANOVA results for Rt.

Source	DF	Seq SS	Adj SS	Adj MS	F	P
Main Effects	3	0.714	0.714	0.238	122.68	0.000
Vc	1	0.004	0.004	0.004	1.90	0.240
f	1	0.709	0.709	0.709	365.37	0.000
ap	1	0.001	0.0014	0.001	0.76	0.433
2-Way Int.	3	0.027	0.027	0.009	4.60	0.087
Vc*f	1	0.003	0.003	0.003	1.55	0.281
Vc*ap	1	0.000	0.000	0.000	0.02	0.895
f*ap	1	0.024	0.024	0.024	12.23	0.025
3-Way Int.	1	0.003	0.003	0.003	1.47	0.292
Vc*f*ap	1	0.003	0.003	0.003	1.47	0.292
Curvature	1	0.004	0.004	0.004	2.01	0.230
Residual Error	4	0.008	0.008	0.002		
Pure Error	4	0.008	0.008	0.002		
Total	12	0.755				

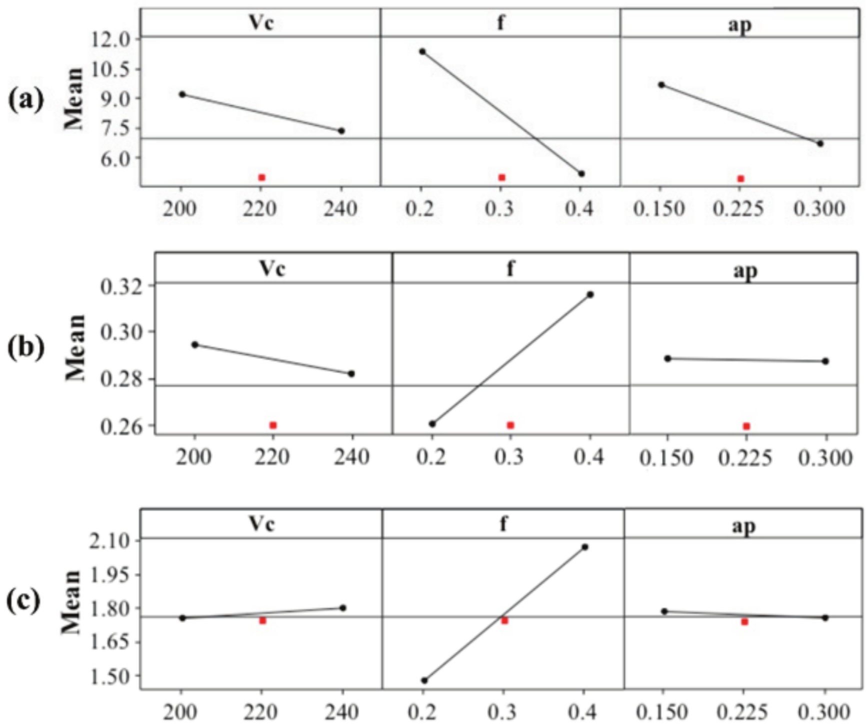

FIGURE 3.
Main effect plots for a) Tool life, T; b) Roughness, Ra and; c) Roughness, Rt.

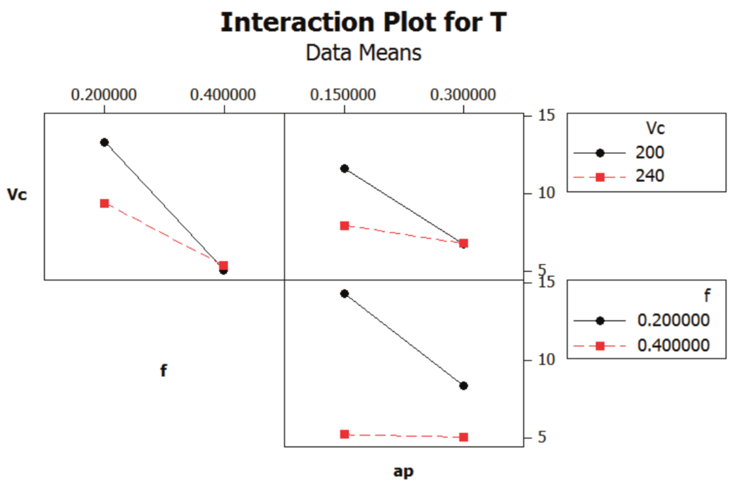

FIGURE 4.
Interaction Plot for T.

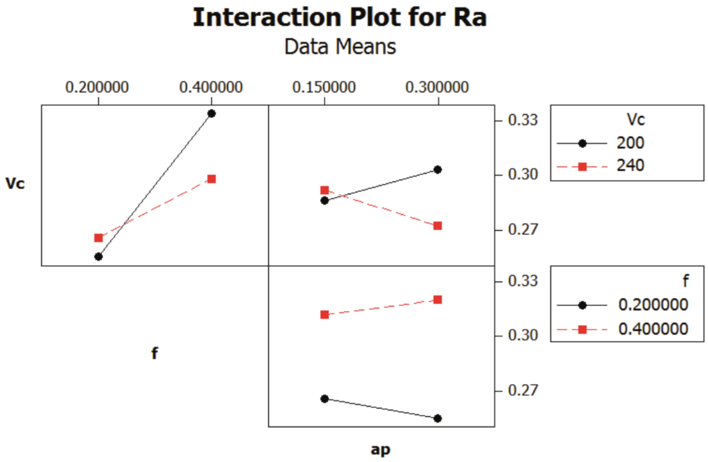

FIGURE 5.
Interaction Plot for Ra.

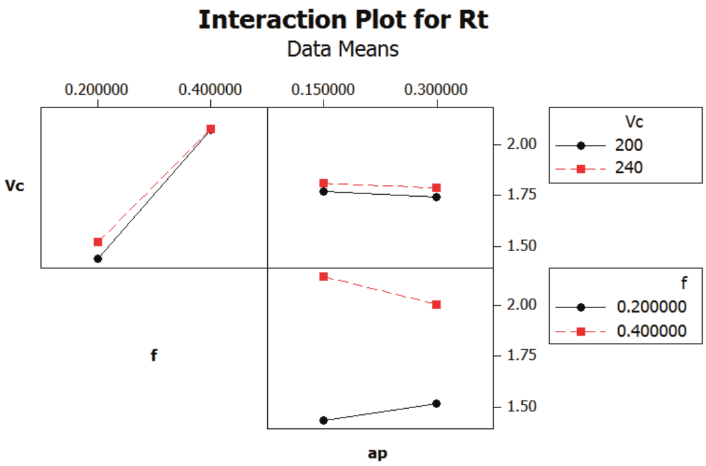

FIGURE 6.
Interaction Plot for Rt.

TABLE 9.
ANOVA results for T.

Source	DF	Seq SS	Adj SS	Adj MS	F	P
Regression	9	240.959	240.959	26.773	761.75	0.000
Linear	3	165.889	165.889	55.296	1573.29	0.000
Vc	1	10.121	10.121	10.121	287.96	0.000
f	1	127.442	127.442	127.442	3626.00	0.000
ap	1	28.325	28.325	28.325	805.91	0.000
Square	3	42.873	42.873	14.291	406.61	0.000
Vc^2	1	9.815	16.977	16.997	483.02	0.000
f^2	1	25.249	28.953	28.953	823.77	0.000
ap^2	1	7.809	7.809	7.809	222.18	0.000
Interaction	3	32.197	32.197	10.732	305.36	0.000
Vc*f	1	8.989	8.989	8.989	255.75	0.000
Vc*ap	1	6.734	6.734	6.734	191.61	0.000
f*ap	1	16.474	16.474	16.474	468.71	0.000
Residual	9	0.316	0.316	0.035		
Lack-of-Fit	5	0.246	0.246	0.049	2.78	0.172
Pure Error	4	0.071	0.071	0.018		
Total	18	241.275				

The hessian matrix was constructed from the quadratic models of the responses. Using the Minitab® software, the eigenvalues were calculated and analyzed. According to the eigenvalues, the T function is convex; Ra and Rt are saddle. So, with the eigenvalues and calculated stationary points from Table 12, it is possible to verify that the stationary point from T is a minimal point and Ra and Rt are border points.

TABLE 10.
ANOVA results for Ra.

Source	DF	Seq SS	Adj SS	Adj MS	F	P
Regression	9	0.019	0.019	0.002	85.54	0.000
Linear	3	0.012	0.012	0.004	159.37	0.000
Vc	1	0.001	0.001	0.001	29.87	0.000
f	1	0.011	0.011	0.011	448.17	0.000
ap	1	0.000	0.000	0.000	0.05	0.829
Square	3	0.005	0.005	0.002	71.10	0.000
Vc^2	1	0.000	0.000	0.000	12.36	0.007
f^2	1	0.000	0.000	0.000	2.17	0.175
ap^2	1	0.005	0.005	0.005	210.63	0.000
Interaction	3	0.002	0.002	0.001	26.14	0.000
Vc*f	1	0.001	0.001	0.001	44.10	0.000
Vc*ap	1	0.001	0.001	0.001	27.85	0.001
f*ap	1	0.000	0.000	0.000	6.46	0.032
Residual	9	0.000	0.000	0.000		
Lack-of-Fit	5	0.000	0.000	0.000	1.85	0.286
Pure	4	0.000	0.000	0.000		
Total	18	0.019				

TABLE 11.
ANOVA results for Rt.

Source	DF	Seq SS	Adj SS	Adj MS	F	P
Regression	9	1.372	1.372	0.152	21.90	0.000
Linear	3	1.234	1.234	0.411	59.06	0.000
Vc	1	0.011	0.011	0.011	1.53	0.248
f	1	1.209	1.209	1.209	173.6	0.000
ap	1	0.014	0.014	0.014	2.07	0.184
Square	3	0.112	0.112	0.037	5.34	0.022
Vc^2	1	0.014	0.005	0.005	0.72	0.418
f^2	1	0.095	0.097	0.097	13.99	0.005
ap^2	1	0.002	0.002	0.002	0.32	0.588
Interaction	3	0.027	0.027	0.009	1.28	0.338
Vc*f	1	0.003	0.003	0.003	0.43	0.527
Vc*ap	1	0.000	0.000	0.000	0.01	0.943
f*ap	1	0.024	0.024	0.024	3.41	0.098
Residual	9	0.063	0.063	0.007		
Lack-of-Fit	5	0.055	0.055	0.011	5.66	0.059
Pure	4	0.008	0.008	0.002		
Total	18	1.435				

TABLE 12.
Stationary points.

T	Ra	Rt
-0.066336	1.581860	1.112008
0.552279	0.732168	-1.867590
-0.007640	0.295808	-3.459571

In this study, it was found that the residuals of the models obtained for the surface roughness and tool life have normal distributions. According to the recommendations (Taguchi, 1986), Myers (1999) conducted a residual analysis of the responses. Residuals are the differences between two or more observations and their average.

The normal probability plot was drawn for residuals as shown in Figure 8a, b and c. It was observed that the points are distributed over the line and P-value of normality test was more than 5%, but the residuals are normally distributed; and the residues shown to be independently and random. Thus, it can be seen that the models were satisfactory. In the P-value hypothesis test, the null hypothesis could not be rejected, so proposed models are adequate.

In order to perform a multiobjective analysis on the controllable variables (Vc, f and ap), the Desirability method was used; with the main objective of maximizing T and minimizing Ra and Rt. The desirability is a multiobjective method capable of evaluating a set of responses simultaneously, and allowing the determination of the most desirable set of conditions for the studied properties (Derringer & Suich, 1980). The optimal points achieved by desirability method for each variable are shown in Figure 9.

With the achieved results, it is possible to verify the robustness of the method to define optimal points for the tool life, minimizing the roughness. The use of desirability is very useful in the optimization processes, as well as in the practical application of this work focusing on the production in industry.

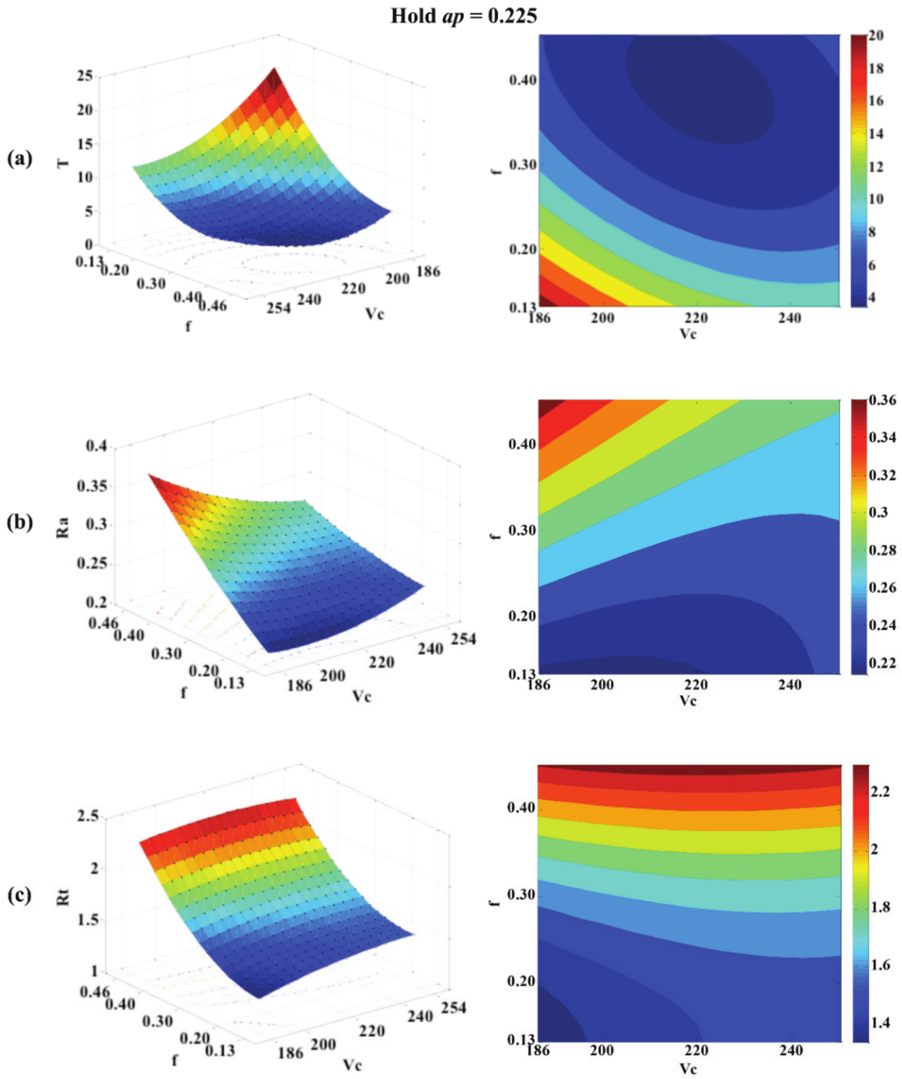

FIGURE 7.
Response surfaces and contour plots for a) T; b) Ra and; c) Rt.

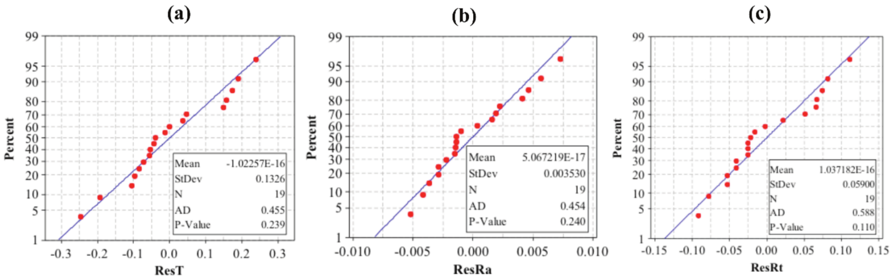

FIGURE 8.
Residual analysis for (a) T; (b) Ra and; (c) Rt.

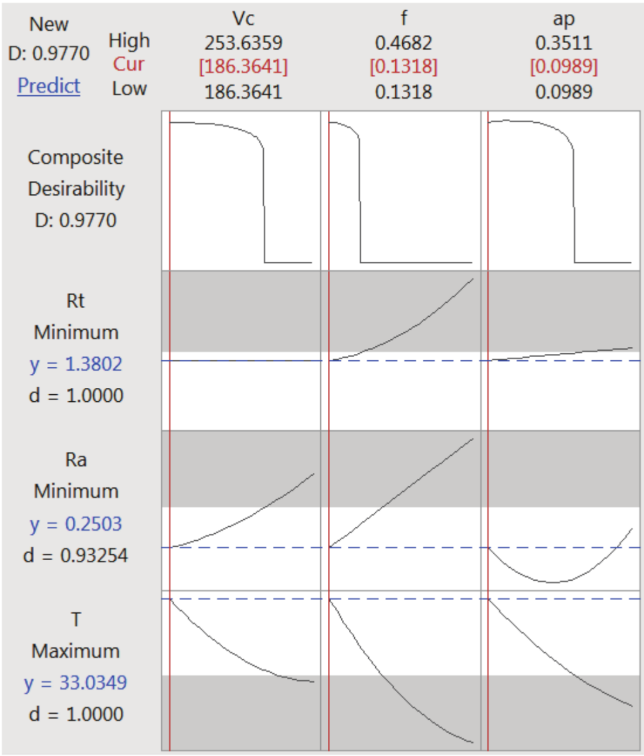

FIGURE 9.
Desirability optimal results for responses.

Conclusion

The complete models obtained by RSM provided excellent (97.69%) explanation for the adjusted parameters of the responses, which demonstrates that the breakthrough factors, ap and Vc, as well as their interactions, have a considerable influence on surface roughness Ra and Rt and T parameters. As they exert significant influence on T, an increase in any of them contributes to the reduction of the cutting tool's life.

Thus, the methodology presented herein proved to be adequate for a turning process optimization. Also, this approach can be applied in experiments with cutting parameters as well.

Acknowledgements

The authors would like to thanks Capes, CNPQ and Fapemig for the support in this research.

References

Bouacha, K., Yallese, M. A., Khamel, S., & Belhadi, S. (2014). Analysis and optimization of hard turning operation using cubic boron nitride tool. International Journal of Refractory Metals and Hard Materials, 45, 160-178. doi: 10.1016/j.ijrmhm.2014.04.014

Chinchanikar, S., & Choudhury, S. K. (2015). Machining of hard steel – experimental investigations, performance modeling and cooling techniques: a review. International Journal of Machine Tools and Manufacture, 89, 95-109. doi: 10.1016/j.ijmachtools.2014.11.002

Davim, J. P. (2011). Machining of hard materials. London, GB: Springer. doi: 10.1007/978-1-84996-450-0

Derringer, G., & Suich, R. (1980). Simultaneous optimization of several response variables. Journal of Quality Technology, 12(4), 214-219. doi: 10.1080/00224065.1980.11980968

Ferreira, R., Řehoř, J., Lauro, C. H., Carou, D., & Davim, J. P. (2016). Analysis of the hard turning of AISI H13 steel with ceramic tools based on tool geometry: surface roughness, tool wear and their relation. Journal of the Brazilian Society of Mechanical Sciences and Engineering, 38(8), 2413-2420. doi: 10.1007/s40430-016-0504-z

Gheshlaghi, R., Scharer, J. M., Moo-Young, M., & Douglas, P. L. (2008). Application of statistical design for the optimization of amino acid separation by reverse-phase HPLC. Analytical Biochemistry, 383(1), 93-102. doi: 10.1016/j.ab.2008.07.032

Grzesik, W., & Wanat, T. (2006). Surface finish generated in hard turning of quenched alloy steel parts using conventional and wiper ceramic inserts. International Journal of Machine Tools & Manufacture, 46(15), 1988-1995. doi: 10.1016/j.ijmachtools.2006.01.009

Grzesik, W., & Zak, K. (2012). Modification of surface finish produced by hard turning using superfinishing and burnishing operations. Journal of Materials Processing Technology, 212(1), 315-322. doi: 10.1016/j.jmatprotec.2011.09.017

Montgomery, D. C. (2008). Design and analysis of experiments. New York, NY: John Wiley & Sons.

Myers, R. H. (1999). Response surface methodology-current status and future directions. Journal of Quality Technology, 31(1), 30-44. doi: 10.1080/00224065.1999.11979891

Ohale, P. E., Uzoh, C. F., & Onukwuli, O. D. (2017). Optimal factor evaluation for the dissolution of alumina from Azaraegbelu clay in acid solution using RSM and ANN comparative analysis. South African Journal of Chemical Engineering, 24, 43-54. doi: 10.1016/j.sajce.2017.06.003

Paiva, A. P., Ferreira, J. R., & Balestrassi, P. P. (2007). A multivariate hybrid approach applied to AISI 52100 hardened steel turning optimization. Journal of Materials Processing Technology, 189(1-3), 26-35. doi: 10.1016/j.jmatprotec.2006.12.047

Pontes, F. J., Silva, M. B., Ferreira, J. R., Paiva, A. P., Balestrassi, P. P., & Schönhorst, G. B. (2010). A DOE based approach for the design of RBF Artificial Neural Networks applied to prediction of surface roughness in AISI 52100 hardened steel turning. Journal of the Brazilian Society of Mechanical Sciences and Engineering, 32(5), 3-510. doi: 10.1590/s1678-58782010000500010

Santhanakumar, M., Adalarasan, R., Siddharth, S., & Velayudham, A. (2016). An investigation on surface finish and flank wear in hard machining of solution treated and aged 18% Ni maraging steel. Journal of the Brazilian Society of Mechanical Sciences and Engineering, 39(6), 2071-2084. doi: 10.1007/s40430-016-0572-0

Scandiffio, I., Diniz, A. E., & Souza, A. F. (2016). Evaluating surface roughness, tool life, and machining force when milling free-form shapes on hardened AISI D6 steel. International Journal of Advanced Manufacturing Technology, 82(9-12), 2075-2086. doi: 10.1007/s00170-015-7525-0

Shihab, S. K., Khan, Z. A., Mohammad, A., & Siddiquee, A. N. (2014a). A review of turning of hard steels used in bearing and automotive applications. Production & Manufacturing Research, 2(1), 24-49. doi: 10.1080/21693277.2014.881728

Shihab, S. K., Khan, Z. A., Mohammad, A., & Siddiqueed, A. N. (2014b). RSM based study of cutting temperature during hard turning with multilayer coated carbide insert. Procedia Materials Science, 6, 1233-1242. doi: 10.1016/j.mspro.2014.07.197

Suleyman, N., Yaldiz, S., & Turkes, E. (2011). Optimization of tool geometry parameters for turning operations based on the response surface methodology. Measurement, 44(3), 580-587. doi: 10.1016/j.measurement.2010.11.018

Taguchi, G. (1987). System of experimental design (Vol. 1-2). New York, NY: Kraus International Publications.

Zhang, X. P., Liu, C. R., & Yao, Z. (2007). Experimental study and evaluation methodology on hard surface integrity. International Journal of Advanced Manufacturing Technology, 34(1-2), 141-148. doi: 10.1007/s00170-006-0575-6